

Impact of loading amount of P_4O_{10} on CO_2 reduction performance of P_4O_{10}/TiO_2 with H_2O extending absorption range from ultraviolet to infrared light

Abstract

The purpose of this study is to clarify the impact of loading amount of P_4O_{10} on the CO_2 reduction performance when P_4O_{10}/TiO_2 is used as the photocatalyst under the infrared light (IR) illumination condition. The CO_2 reduction performance with H_2O over P_4O_{10}/TiO_2 has been investigated under the illumination conditions with ultra violet light (UV) + visible light (VIS) + IR, VIS + IR and IR only. The ratio of CO_2/H_2O has been varied from 1:0.5 to 1:4 in this study. The prepared P_4O_{10}/TiO_2 film has been characterized by SEM and EPMA. As a result, it is revealed that the coated P_4O_{10}/TiO_2 film having teeth-like shape is formed on the netlike glass fiber irrespective of the amount of P_4O_{10} loaded. The distribution of P_4O_{10} becomes more uniform under the small loading amount. The light absorption performance of TiO_2 film extends to VIS and IR by loading P_4O_{10} irrespective of the loading amount of P_4O_{10} . The CO_2 reduction performance for the molar ratio of $CO_2/H_2O = 1:1$ is the highest among different molar ratios under the illumination condition with UV + VIS + IR, VIS + IR, and IR only irrespective of loading amount of P_4O_{10} for P_4O_{10}/TiO_2 film. This result matches with the theoretical molar ratio to produce CO according to the CO_2/H_2O reaction scheme. The CO_2 reduction performance for the weight percentage of P_4O_{10} of 1.1 wt% is the highest under all illumination conditions of UV + VIS + IR, VIS + IR, and IR only. The molar quantity of CO per unit weight of photocatalyst for P_4O_{10}/TiO_2 film of 394.6 $\mu\text{mol/g}$ is obtained under the illumination condition of IR only.

Keywords: CO_2 reduction, P_4O_{10}/TiO_2 photocatalyst, Optimum loading amount, Visible light, Infrared light.

Introduction

The global average concentration of CO_2 in the atmospheric air has been increasing up to 416 ppmV in July 2022, indicating that it is an increase of 76 ppmV compared to 1980.¹ It is necessary to develop CO_2 reduction technologies to prevent the continuous rise of global temperature.

It is known that CO_2 can be converted/reduced into fuel species such as CO, CH_4 , CH_3OH etc. by photocatalyst.²⁻⁵ TiO_2 can work under the ultra violet light (UV) illumination condition only. It is known that UV light accounts for 4 % only in sunlight.⁶ If we could use the visible light (VIS) and infrared light (IR) which accounts for 44 % and 52 % of solar energy reaching the earth respectively⁶ for the photocatalytic CO_2 reduction, it would promote the photocatalytic CO_2 reduction performance remarkably. Moreover, it can be said that the whole solar energy can be utilized for the photocatalytic CO_2 reduction.

Regarding the photocatalytic researches on extending the absorption performance of the light wavelength from UV to VIS, many trials have been reported.⁷⁻¹⁶ One of the major attempts is a metal doping. Cu is a popular metal dopant. Cu/TiO_2 has performed the absorption of light whose wavelength is ranged from 400 nm to 800 nm and produced CO of 0.5 $\mu\text{mol/g}$ and H_2 of 4 $\mu\text{mol/g}$.⁷ Cu_2O/TiO_2 has produced CO of 80 $\mu\text{mol/g}$ under the Xe lamp illumination condition whose wavelength of light is ranged from 320 nm to 780 nm.⁸ Cu ultrathin TiO_2 which absorbs the light whose wavelength is ranged from 400 nm to 800 nm has produced CO of 7 $\mu\text{mol/g}$.⁹ Cu_2O clusters/ TiO_2 nanosheet absorbing the light whose wavelength is ranged from 300 nm to 600 nm has produced CH_4 of 225.6 $\mu\text{mol/g}$, resulting

from that the coordination bonds of C=O and C-O could accelerate the photogenerated electron transfer to CO_2^{10} . Pd is also adopted as a metal dopant. Pd/TiO_2 nanowire has performed the absorption of light whose wavelength is ranged from 350 nm to 700 nm, producing CH_4 yield of 26.7 $\mu\text{mol/g}$ and CO yield of 50.4 $\mu\text{mol/g}$.¹¹ Pd/TiO_2 (3 wt% of Pd) extending the absorption limit up to 700 nm has produced CH_4 of 4.2 $\mu\text{mol/g}$ and CO of 2.1 $\mu\text{mol/g}$.¹² Zn and Pd co-modified TiO_2 has exhibited CH_4 yield of 53.3 $\mu\text{mol/g}$ under the illumination condition of 500 W Xe arc lamp whose wavelength of light is ranged from 290 nm to 800 nm.¹³ It is known that Pt is another candidate as a metal dopant. Graphene-wrapped Pt/TiO_2 has shown the light absorption from 300 nm to 750 nm, resulting in CO production of 320 $\mu\text{mol/g}$ and CH_4 production of 45 $\mu\text{mol/g}$.¹⁴ Pt/TiO_2 synthesized by thermal hydrolysis of two different precursors has exhibited the light absorption from 200 nm to 700 nm and produced CH_4 of 0.73 $\mu\text{mol/g}$ and CO of 0.17 $\mu\text{mol/g}$.¹⁵ Nanocrystals-supported $PtRu/TiO_2$ has performed the light absorption from 300 nm to 750 nm and produced CH_4 of 300 $\mu\text{mol/g}$.¹⁶

Regarding the photocatalytic researches on extending the absorption performance of light wavelength up to IR, there are some researches relating the photocatalyst except for TiO_2 .¹⁷⁻²¹ $W_{18}O_{49}/g-C_3N_4$ composite has displayed the CO production of 45 $\mu\text{mol/g}$ and the CH_4 production of 28 $\mu\text{mol/g}$ under the illumination condition whose wavelength is ranged from 200 nm to 2400 nm.¹⁷ WS_2/Bi_2S_3 nanotube has exhibited the absorption of VIS and near IR light (wavelength: 420 nm – 1100 nm), which has produced CH_3OH of 28 $\mu\text{mol/g}$ and C_2H_5OH of 25 $\mu\text{mol/g}$.¹⁸ $CuInZnS$ decorated $g-C_3N_4$ has exhibited the absorption performance of light whose wavelength is

ranged from 200 nm to 1000 nm, performing the CO production of 38 $\mu\text{mol/g}$.¹⁹ Hierarchical $ZnIn_2S_4$ nanorod prepared by solvothermal method has produced CO of 54 $\mu\text{mol/g}$ and CH_4 of 9 $\mu\text{mol/g}$.²⁰ The plasmonic semiconductor constructed by coupling pyroelectric black phosphorus (BP) and plasmonic WO has exhibited CO production of 78 $\mu\text{mol/g}$ under VIS and near-infrared light (NIR) illumination condition.²¹ Under the VIS-NIR illumination condition, the plasmonic thermal effect of WO can bring the local temperature rise up to 86 °C, and the thermal radiation can trigger the pyroelectric BP to generate carriers and electric field promoting electron transfer to WO, which promotes the CO_2 reduction performance under the VIS-NIR illumination condition.

Though several studies on extending the absorbed light of wavelength up to IR have been reported, there is no report investigating the extension of light absorption performance of TiO_2 up to IR. Therefore, this study attempts to extend the light absorption performance of TiO_2 up to IR. According to the previous report,²² the composite photocatalyst of BP and $g-C_3N_4$ has performed the H_2 production from H_2O under VIS and near IR illumination condition. Phosphorus (P) has a layer structure absorbing the light whose wavelength is ranged from UV to IR. Therefore, the purpose of this study is to clarify the impact of loading amount of P on the CO_2 reduction performance of P/TiO_2 under IR illumination condition. This study investigates the CO_2 reduction performance of P/TiO_2 changing the wavelength of illuminated light by UV + VIS + IR, VIS + IR and IR only.

For the photocatalytic CO_2 reduction reaction, a reductant is important since it is a partner for CO_2 . It is found from some review papers²³⁻²⁵ that H_2O is a popular reductant. According to the past studies,²⁶⁻²⁸ we can show the reaction scheme of CO_2 reduction with H_2O as below:

<Photocatalytic reaction>



<Oxidation>



<Reduction>



In this study, The CO_2 reduction performance with H_2O over P/TiO_2 has been investigated under the illumination conditions of UV + VIS + IR, VIS + IR and IR only. The ratio of CO_2/H_2O has been set at 1:0.5, 1:1, 1:2 and 1:4 to determine the optimum molar ratio of CO_2/H_2O over P/TiO_2 . According to the reaction scheme to reduce CO_2 with H_2O as shown above, the theoretical molar ratio of CO_2/H_2O to produce CO or CH_4 should be 1:1 or 1:4, respectively. In addition, this study has investigated the impact of loading amount of P on the CO_2 reduction performance of P/TiO_2 . In this study, P_4O_{10} is loaded as a type of P on TiO_2 identified by the previous study by the authors.²⁹

Materials and method

The preparation procedure of P_4O_{10}/TiO_2 film

The TiO_2 film used in this study was prepared by sol-gel and dip-coating process.³⁰⁻³² $[(CH_3)_2CHO]_4Ti$ (purity: 95 wt%, producer: Nacalai Tesque Co., Kyoto, Japan) of 0.3 mol, anhydrous C_2H_5OH (purity: 99.5 wt%, producer: Nacalai Tesque Co., Kyoto, Japan) of 2.4 mol, distilled water of 0.3 mol, and HCl (purity: 35 wt%, producer:

Nacalai Tesque Co., Kyoto, Japan) of 0.07 mol were mixed to prepare the TiO_2 sol solution. The TiO_2 film was coated on a netlike glass fiber (SILLIFGLASS U, producer: Nihonmuki Co., Tokyo, Japan) via sol-gel and dip-coating processes. The glass fiber with a diameter of about 10 μm , which is weaved as a net, is assembled to be the diameter of about 1 mm. According to the specification on netlike glass fiber, the porous diameter of glass fiber and the specific surface area is approximately 1 nm and 400 m^2/g , respectively. The netlike glass fiber consists of SiO_2 of 96 wt%. The netlike glass fiber has the opening space of about 2 mm \times 2 mm. The netlike glass fiber has a porous characteristic, resulting that the netlike glass fiber can trap the TiO_2 film easily via sol-gel and dip-coating processes. In addition, it can be expected that CO_2 and reductant such as H_2O and NH_3 are more easily absorbed by the prepared photocatalyst since the netlike glass fiber has a porous characteristic. The netlike glass fiber is cut to be the disc form with the diameter of 50 mm and the thickness of 1 mm. The dipping speed of the netlike glass disc into TiO_2 sol solution was controlled at 1.5 mm/s and the speed of drawing up was fixed at 0.22 mm/s. Then, the film was dried out and fired by controlling a firing temperature (FT) and a firing duration time (FD), resulting that the TiO_2 film is fastened on the base material. The FT and FD were set at 623 K and 180 s, respectively.

In this study, P_4O_{10} which had been identified by XPS analysis²⁹ was made from the red P by a mechanical synthesis.³³ The red P (average diameter: 75 μm ; producer: Nacalai Tesque Co., Kyoto, Japan) was filled in a ball mill crusher (AV-1, producer: Asahi Rika Factory, Chiba, Japan) with Al_2O_3 ball whose diameter of 3/8 inch (HD-10, producer NIKKATO CORPORATION, Osaka, Japan). The weight ratio of Al_2O_3 balls to red P particles in the ball mill crusher was set at 20.³³ Rotation with the speed of 600 rpm was kept for 12 hours, after that the P_4O_{10} was prepared.

The prepared P_4O_{10} particles were put into TiO_2 sol solution and mixed with TiO_2 sol solution by a magnetic stirrer for 60 min. After that, the netlike glass disc was immersed into this mixed solution. The following process was same as explained above. The weight ratio of P_4O_{10} to TiO_2 was changed and confirmed by EPMA analysis quantitatively. Figure 1 shows the photo of prepared P_4O_{10}/TiO_2 coated on netlike glass disc.



Figure 1 Photo of prepared P_4O_{10}/TiO_2 .

The characterization procedure of P_4O_{10}/TiO_2 film

The characteristics of external and crystal structure of P_4O_{10} loaded on TiO_2 film were evaluated by SEM (JXA-8530F, producer: JEOL Ltd., Tokyo, Japan) and EPMA (JXA-8530F, producer: JEOL Ltd., Tokyo, Japan).³⁰⁻³² The netlike glass disc which was used for a base material to coat TiO_2 film cannot conduct electricity, resulting that we deposited the vaporized Pt by means of the Pt coating device (JEC-1600, producer: JEOL Ltd., Tokyo, Japan) on the surface of the TiO_2 film before the characterization. The deposited Pt has the thickness of 15 nm. The electrode emitted the electrons to the sample by setting the acceleration voltage and the current at 15 kV and 3.0×10^{-8} A respectively, to analyze the external structure of TiO_2 film by means of SEM. We analyzed the character X-ray by means of EPMA at the same time, resulting that the amount of chemical element was estimated based on the relationship between the character X-ray energy and the atomic number. The space resolution of SEM and EPMA is 10 μ m. The structure of prepared P_4O_{10}/TiO_2 photocatalyst was analyzed by the EPMA.

CO_2 reduction experiment

Figure 2 illustrates the experimental apparatus. The reactor consists of a stainless tube with a scale of 100 mm (H) \times 50 mm ($I.D.$), TiO_2 film or P_4O_{10}/TiO_2 which is coated on the netlike glass disc with a scale of 50 mm (D) \times 1 mm (t) positioned on the Teflon cylinder with a scale of 50 mm (H) \times 50 mm (D), a quartz glass disc having a scale of 84 mm (D) \times 10 mm (t), a sharp cut filter removing the wavelength of light which is below 400 nm (SCF-49.5C-42L, producer: SIGMA KOKI CO.LTD., Tokyo, Japan) or 800 nm (ITF-50C-85IR, producer: SIGMA KOKI CO.LTD., Tokyo, Japan), a 150 W Xe lamp (L2175, producer: Hamamatsu Photonics K. K.), mass flow controller and CO_2 gas cylinder (purity: 99.995 vol%) in case of CO_2 reduction experiment with H_2O .³⁰ The reactor size for charging

CO_2 is 1.25×10^{-4} m 3 . The light of Xe lamp located on the stainless tube is illuminated toward P_4O_{10}/TiO_2 film passing the sharp cut filter and the quartz glass disc positioned on the top of the stainless tube. The wavelength of light illuminated from Xe lamp is distributed from 185 nm to 2000 nm. The sharp cut filter can remove the UV from the Xe lamp, providing the wavelength of light illuminating P_4O_{10}/TiO_2 film ranged from 401 nm to 2000 nm or 801 nm to 2000 nm.³⁴ Figure 3 exhibits the light transmittance data of sharp cut filter cutting the wavelength below 400 nm to clarify the light illumination condition as an example. The mean light intensity of light illuminated from Xe lamp from 185 nm to 2000 nm is 72.0 mW/cm 2 , that from 401 nm to 2000 nm is 60.0 mW/cm 2 , and that from 801 nm to 2000 nm is 51.0 mW/cm 2 . After filling CO_2 gas with the purity of 99.995 vol% in the reactor pre-vacuumed by means of a vacuum pump for 15 min, we closed the valves which were installed at the inlet and the outlet of reactor during CO_2 reduction experiment with H_2O . We confirmed the pressure and gas temperature at 0.1 MPa and 298 K, respectively in the reactor. After that, the distilled H_2O was injected into the reactor via the gas sampling tap, and the Xe lamp was turned on at the same time. We changed the amount of injected H_2O according to the molar ratio. The injected H_2O solution was vaporized by the heat of IR components illuminated from the Xe lamp. We confirmed that the temperature in the reactor attained at 343 K within an hour, and we kept at approximately 343 K during the CO_2 reduction experiment. We changed the molar ratio of CO_2/H_2O by 1:0.5, 1:1, 1:2 and 1:4. We extracted the reacted gas filled in the reactor by means of gas syringe via gas sampling tap and we analyzed using a FID gas chromatograph (GC353G, producer: GL Science) and a methanizer (MT221, producer: GL Science). The minimum resolution of FID gas chromatograph and methanizer is 1 ppmV. The CO_2 reduction experiment was conducted up to 8 hours. Gas sampling was carried out from the start of experiment till 8 hours by 2 hours.

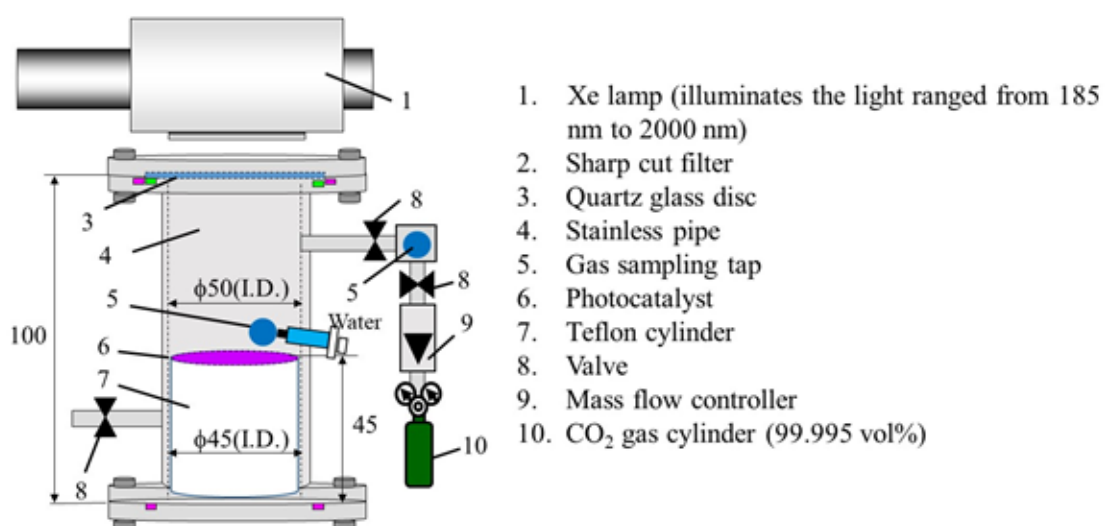


Figure 2 Schematic diagram of experimental apparatus of CO_2 reduction with H_2O . The reactor consists of stainless pipe, TiO_2 film or P_4O_{10}/TiO_2 film photocatalyst located on Teflon cylinder, a quartz glass disc, sharp cut filter, a 150 W Xe lamp, mass flow controller and CO_2 gas cylinder.

Results and discussion

Characterization analysis of P_4O_{10}/TiO_2 film

The observation area which is the center of netlike glass disc having the diameter of 300 μ m was analyzed by EPMA to measure the loading quantity of P_4O_{10} in the TiO_2 film. The ratio of P_4O_{10} to Ti was calculated by averaging the data detected in this area. The weight percentage of P_4O_{10} within P_4O_{10}/TiO_2 film prepared in this

study was 1.1 wt%, 4.2 wt% and 13.4 wt%. Figures 4, 5 and 6 show SEM and EPMA images of P_4O_{10}/TiO_2 film coated on netlike glass disc for the weight percentage of P_4O_{10} of 1.1 wt%, 4.2 wt% and 13.4 wt%, respectively. Black and white SEM images at 1500 times magnification were obtained in this study, which were also used for EPMA analysis. Regarding the EPMA image, the concentrations of each element in observation area are displayed by diverse colors. Light colors, e.g., white, pink, and red indicate a large amount of an

element. On the other hand, dark colors like black and blue indicate a small amount of element. It is observed from Figures 4, 5 and 6 that P_4O_{10}/TiO_2 film having teeth-like shape coated on the netlike glass fiber is formed irrespective of the weight percentage of P_4O_{10} within P_4O_{10}/TiO_2 film. Since the thermal conductivity of Ti and SiO_2 at 600 K are 19.4 W/(m·K) and 1.82 W/(m·K), respectively³⁵, the temperature distribution of TiO_2 solution adhered on the net like glass disc was not even during the firing process. Since thermal expansion and shrinkage around netlike glass fibers occurred, the formation of thermal cracks formed within the TiO_2 film. Therefore, it is believed that TiO_2 film on netlike glass fiber has a teeth-like form. In addition, it is found from Figures 4, 5 and 6 that nanosized P_4O_{10} particles are loaded on TiO_2 film. When the amount of P_4O_{10} increases, it is seen that the gap between the weak and the strong detected P_4O_{10} is bigger. It is thought that the distribution of P_4O_{10} particles in TiO_2 solution might become uneven with the increase of the amount of P_4O_{10} particles during the dipping process for preparation of P_4O_{10}/TiO_2 . Therefore, it can be claimed that it is easy to obtain the uniform distribution of P_4O_{10} under the small amount of P_4O_{10} loading condition. On the other hand, the total weights of P_4O_{10}/TiO_2 which were measured by an electron balance and averaged among 10 samples are 0.002 g, 0.011 g and 0.014 g, respectively.

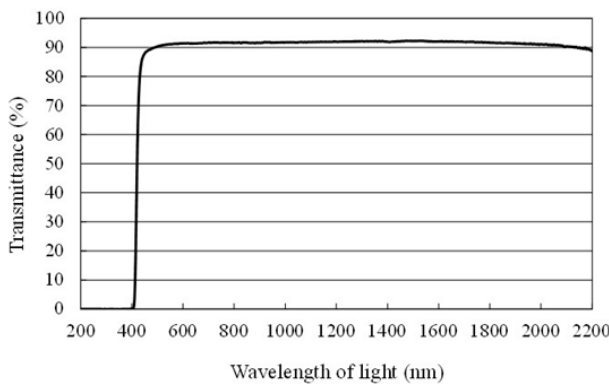


Figure 3 Light transmittance data of sharp cut filter cutting the wavelength below 400 nm.

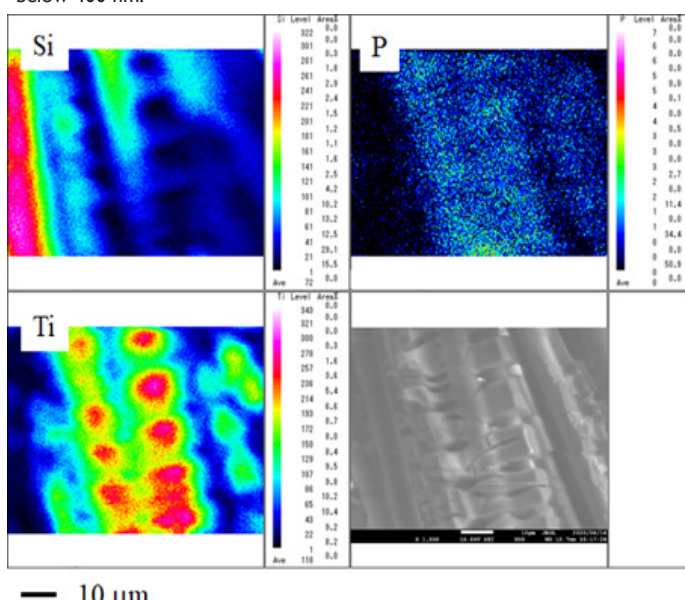


Figure 4 SEM and EPMA results of P_4O_{10}/TiO_2 film coated on netlike glass disc (1.1 wt%).

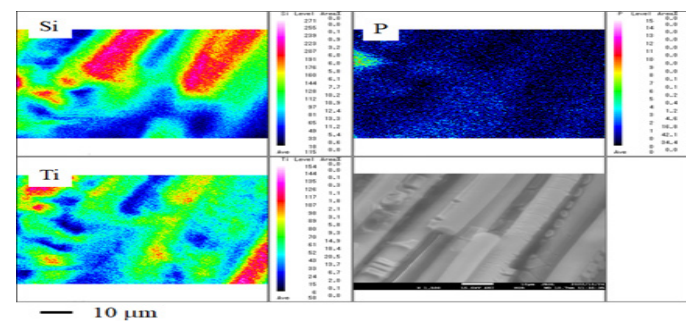


Figure 5 SEM and EPMA results of P_4O_{10}/TiO_2 film coated on netlike glass disc (4.2 wt%).

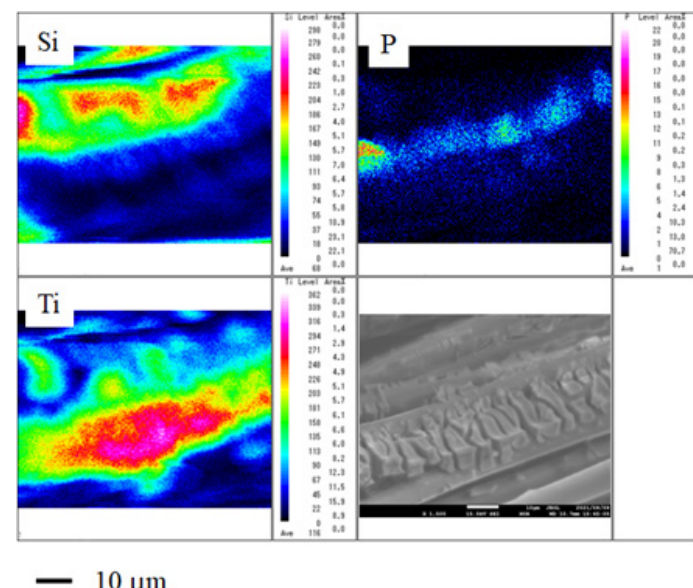


Figure 6 SEM and EPMA results of P_4O_{10}/TiO_2 film coated on netlike glass disc (13.4 wt%).

Comparison of CO_2 reduction performance among different molar ratios of CO_2/H_2O and different loading amounts of P_4O_{10} under the illumination condition with UV + VIS + IR

Figures 7, 8 and 9 show the comparison of concentration change of CO formed with time for P_4O_{10}/TiO_2 among different molar ratios of CO_2/H_2O changing the weight percentage of P_4O_{10} of 1.1 wt%, 4.2 wt% and 13.4 wt%, respectively, under the illumination condition with UV + VIS + IR. In these figures, this study evaluates the produced CO by the molar quantity of CO per unit weight of photocatalyst ($\mu\text{mol/g}$) quantitatively. The other fuels were not detected. Regarding a blank test, we carried out the same experiment under no Xe lamp illumination condition as a reference test before the experiment. As a result, no fuel was detected during the blank test as we expected. This study conducted that the CO_2 reduction experiment with H_2O without photocatalyst under the illumination condition with UV + VIS + IR. As a result, no fuel has been detected. Regarding the repeatability of experiments, we show the average data of three experiments. After three experiments, the change of surface structure cannot be confirmed by the naked eye. Moreover, we have tried to touch the surface of photocatalyst, resulting that the degradation of surface has not been observed.

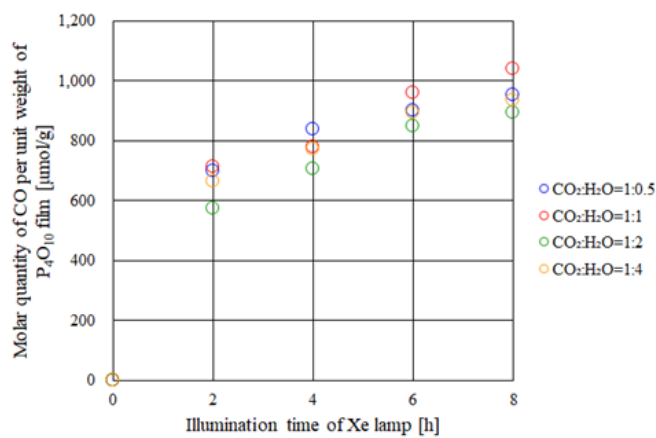


Figure 7 Comparison of molar quantity of CO per unit weight of P_4O_{10}/TiO_2 film among different molar ratios under the illumination condition with UV + VIS + IR (1.1 wt%).

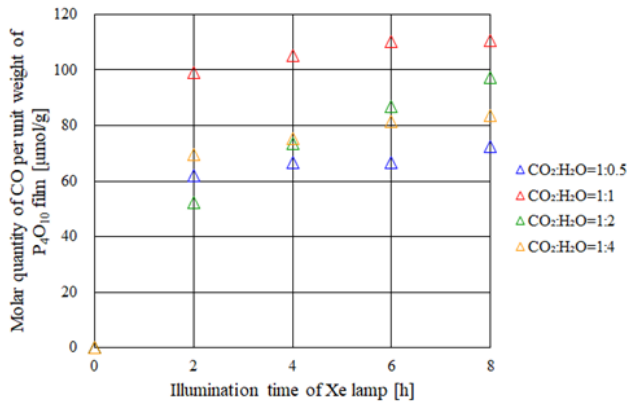


Figure 8 Comparison of molar quantity of CO per unit weight of P_4O_{10}/TiO_2 film among different molar ratios under the illumination condition with UV + VIS + IR (4.2 wt%).

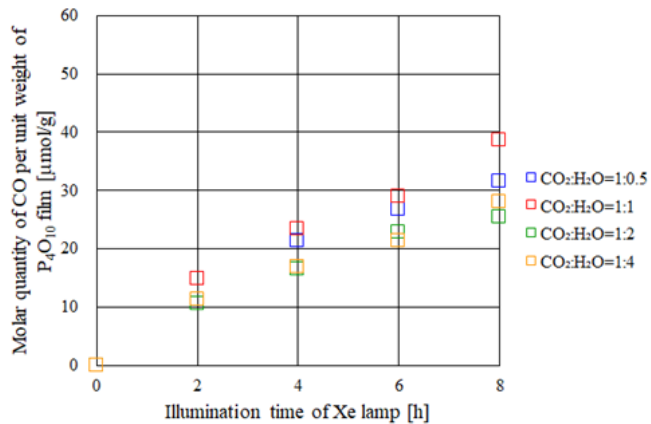


Figure 9 Comparison of molar quantity of CO per unit weight of P_4O_{10}/TiO_2 film among different molar ratios under the illumination condition with UV + VIS + IR (13.4 wt%).

It can be seen from Figures 7, 8 and 9 that the CO_2 reduction performance for the molar ratio of $CO_2:H_2O = 1:1$ is the highest among different molar ratios irrespective of loading amount of P_4O_{10} . The results agreed with the reaction scheme, i.e. Eqs. (1) – (3), that is the theoretical molar ratio to produce CO in case of $CO_2:H_2O$ is

$CO_2:H_2O = 1:1$. Comparing to the CO_2 reduction performance of TiO_2 film under the illumination condition with UV + VIS + IR,²⁹ the superiority of P_4O_{10} has been confirmed. The previous study reported that the highest molar quantity of CO per unit weight of TiO_2 film was $27.5 \mu\text{mol/g}$.²⁹ The highest molar quantity of CO per unit weight of P_4O_{10}/TiO_2 film found in this study was $1038.3 \mu\text{mol/g}$. The reason might be that the light absorption range was extended to IR range.²⁹

Figure 10 shows the comparison of concentration change of CO formed with time among different weight percentages of P_4O_{10} under the illumination condition with UV + VIS + IR. The molar ratio of $CO_2:H_2O$ was 1:1 in this figure. According to Figure 10, it is revealed that the CO_2 reduction performance for the P_4O_{10} weight percentage of 1.1 wt% is the highest. In addition, as shown in EPMA image, i.e. Figure 4, the uniform distribution of P_4O_{10} within TiO_2 film was obtained, resulting that the fine network with TiO_2 was constructed, and the light energy absorbed by P_4O_{10} promoted the generation of holes and electrons as well as separation of them.³⁶ It provides the improvement of CO_2 reduction performance of photoacatalyst. Consequently, the highest CO_2 reduction performance is obtained for the weight percentage of P_4O_{10} of 1.1 wt%.

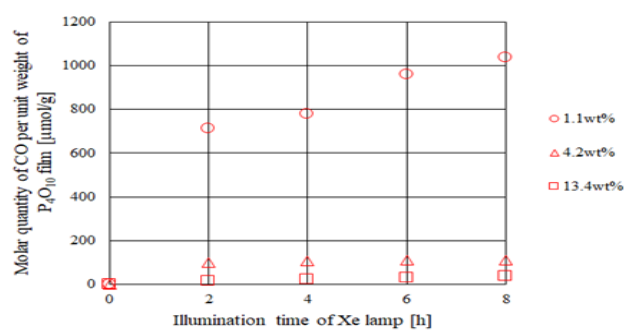


Figure 10 Comparison of molar quantity of CO per unit weight of P_4O_{10}/TiO_2 film among different weight percentages of P_4O_{10} within P_4O_{10}/TiO_2 film under the illumination condition with UV + VIS + IR.

Comparison of CO_2 reduction performance among different molar ratios of $CO_2:H_2O$ and different loading amounts of P_4O_{10} under the illumination condition with VIS + IR

Figures 11, 12 and 13 show the comparison of concentration change of CO formed with time among different molar ratios of $CO_2:H_2O$ changing the weight percentage of P_4O_{10} of 1.1 wt%, 4.2 wt% and 13.4 wt%, respectively, under the illumination condition of VIS + IR. In this study, the other fuels than CO were not detected. The same experiment under no Xe lamp illumination condition as a reference/blank test before the experiment was conducted, resulting that no fuel was detected as expected. In addition to the blank test, the CO_2 reduction experiment with H_2O but without photocatalyst under the illumination condition with VIS + IR was also conducted, resulting that no fuel was detected as expected. Furthermore, no fuel was detected from the CO_2 reduction experiment using TiO_2 film, instead of P_4O_{10}/TiO_2 film with H_2O under the illumination condition with VIS + IR. Therefore, it is confirmed that the CO_2 reduction performance of P_4O_{10}/TiO_2 film is superior to that of TiO_2 film according to Figures 11, 12 and 13. Regarding the repeatability of experiments, the results shown are the average data of three experiments. After three experiments, the change and/or the degradation of surface structure cannot be confirmed by the naked eye.

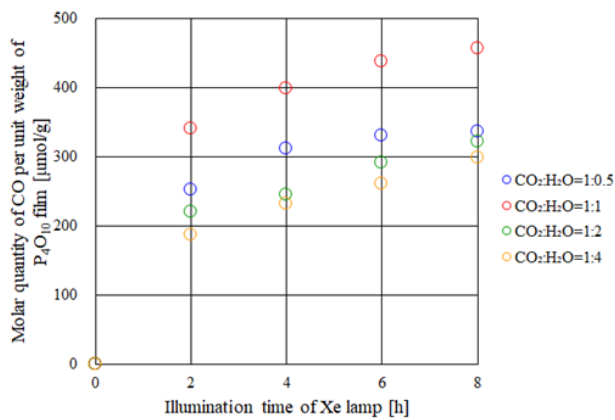


Figure 11 Comparison of molar quantity of CO per unit weight of P_4O_{10}/TiO_2 film among different molar ratios under the illumination condition with VIS + IR (1.1 wt%).

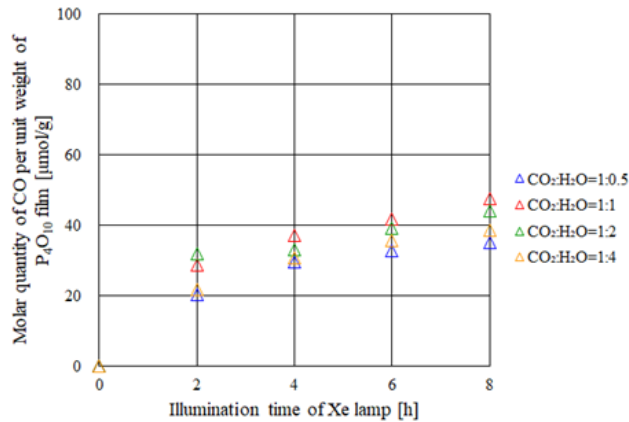


Figure 12 Comparison of molar quantity of CO per unit weight of P_4O_{10}/TiO_2 film among different molar ratios under the illumination condition with VIS + IR (4.2 wt%).

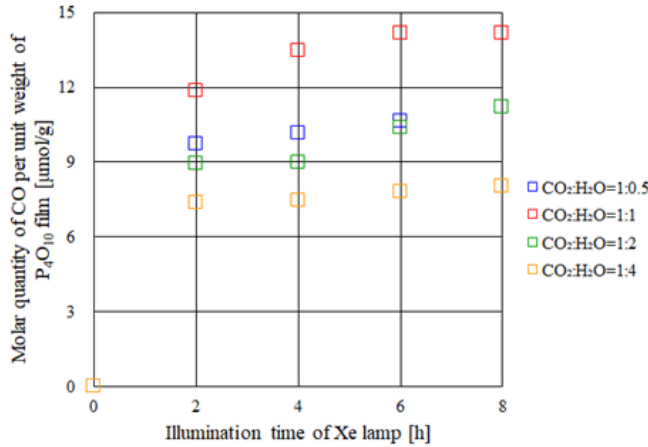


Figure 13 Comparison of molar quantity of CO per unit weight of P_4O_{10}/TiO_2 film among different molar ratios under the illumination condition with VIS + IR (13.4 wt%).

It can be seen from Figures 11, 12 and 13 that the CO_2 reduction performance for the CO_2/H_2O molar ratio of 1:1 is the highest, which agrees with the reaction scheme shown in Eqs. (1) – (3). Namely, the theoretical result in case of TiO_2 is obtained for P_4O_{10}/TiO_2 film with

VIS + IR, which is the same tendency as the illumination with UV + VIS + IR.

Figure 14 shows the comparison of concentration change of CO formed with time among different weight percentages of P_4O_{10} under the illumination condition with VIS + IR. The molar ratio of CO_2/H_2O is 1:1 in this figure. According to Figure 14, it is revealed that the CO_2 reduction performance with the weight percentage of P_4O_{10} of 1.1 wt% is the highest, which is the same as that under the illumination of UV + VIS + IR. The reason is the same as the discussion above for the condition of illumination of UV + VIS + IR. The highest CO_2 reduction performance of 456.5 $\mu\text{mol/g}$ was obtained with the weight percentage of P_4O_{10} of 1.1 wt% under the illumination condition with VIS + IR.

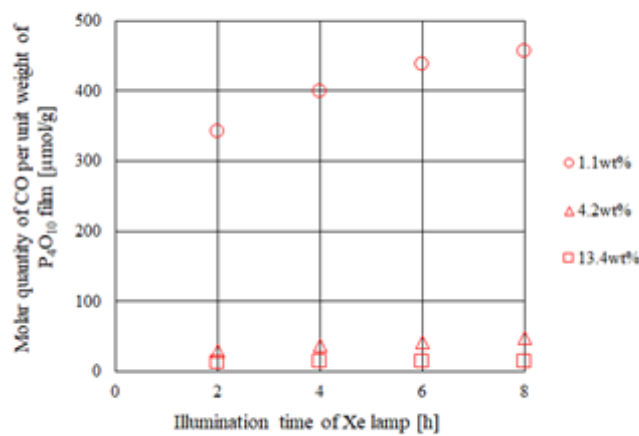


Figure 14 Comparison of molar quantity of CO per unit weight of P_4O_{10}/TiO_2 film among different weight percentages of P_4O_{10} within P_4O_{10}/TiO_2 film under the illumination condition with VIS + IR.

Comparison of CO_2 reduction performance among different molar ratios of CO_2/H_2O and different loading amounts of P_4O_{10} under the illumination condition with IR only

Figures 15, 16 and 17 show the comparison of concentration change of CO formed with time for the P_4O_{10} weight percentage of 1.1 wt%, 4.2 wt% and 13.4 wt%, respectively, under the illumination condition with IR only. In this study, no other fuels (other than CO) were detected. The same experiment under no Xe lamp illumination condition as a reference/blank test before the experiment was conducted in which no fuel was detected as expected. In addition to the blank test, the CO_2 reduction experiment with H_2O but without photocatalyst under the illumination condition with IR only was also conducted. As a result, no fuel was detected as expected. Furthermore, no fuel was detected from the CO_2 reduction experiment using TiO_2 film, instead of P_4O_{10}/TiO_2 film with H_2O under the illumination condition with IR only. Therefore, it is confirmed that the CO_2 reduction performance with P_4O_{10}/TiO_2 film is superior to that with TiO_2 film according to Figures 15, 16 and 17. Regarding the repeatability of experiments, the results shown are the average data of three experiments. After three experiments, the change and/or the degradation of surface structure cannot be confirmed by the naked eye.

It can be seen from Figures 15, 16 and 17 that the CO_2 reduction performance for the CO_2/H_2O molar ratio of 1:1 is the highest among

different molar ratios irrespective of P_4O_{10} loaded, which shows the same tendency as that with the illumination condition of UV + VIS + IR as well as that of VIS + IR.

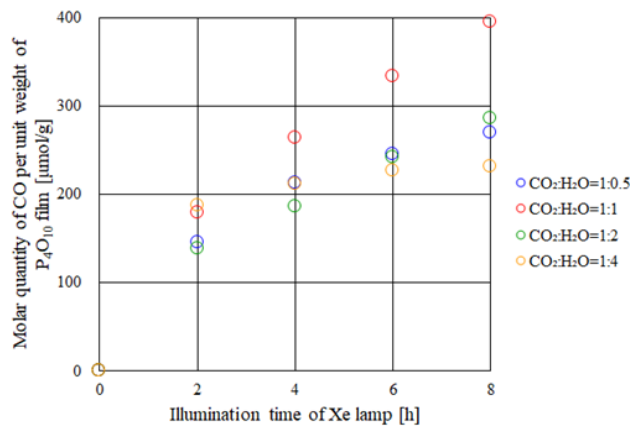


Figure 15 Comparison of molar quantity of CO per unit weight of P_4O_{10}/TiO_2 film among different molar ratios under the illumination condition with IR only (1.1 wt%).

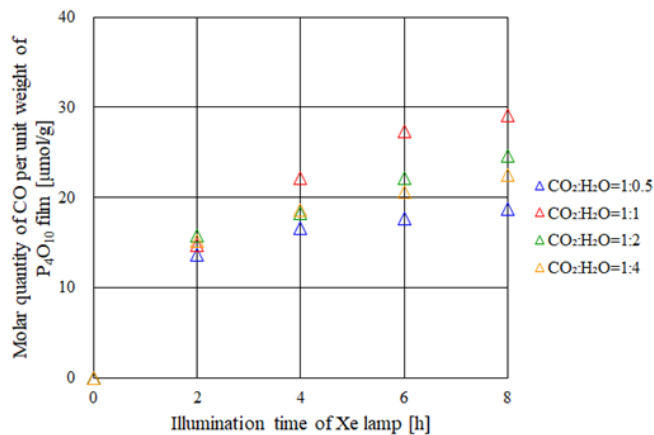


Figure 16 Comparison of molar quantity of CO per unit weight of P_4O_{10}/TiO_2 film among different molar ratios under the illumination condition with IR only (4.2 wt%).

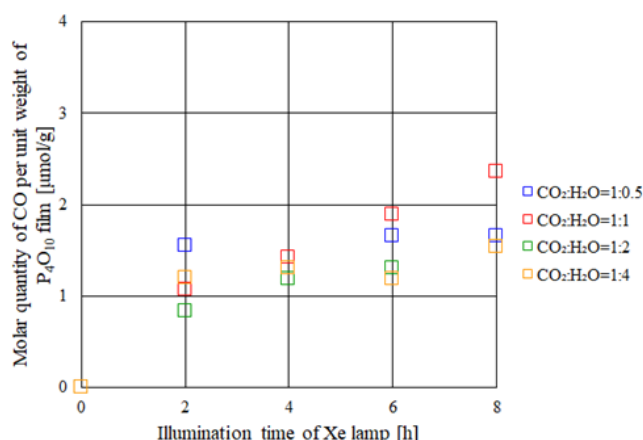


Figure 17 Comparison of molar quantity of CO per unit weight of P_4O_{10}/TiO_2 film among different molar ratios under the illumination condition with IR only (13.4 wt%).

Figure 18 shows the comparison of concentration change of CO formed with time among different weight percentages of P_4O_{10} under

the illumination condition with IR only. The molar ratio of CO_2/H_2O is 1:1 in this figure. According to Figure 18, it is revealed that the CO_2 reduction performance with the P_4O_{10} weight percentage of 1.1 wt% is the highest, which is the same as that under the illumination condition of UV + VIS + IR as well as that of VIS + IR. The reason is thought to be that the distribution of P_4O_{10} is more uniform under the small loading amount of P_4O_{10} as discussed above. The highest molar quantity of CO per unit weight of photocatalyst for P_4O_{10}/TiO_2 film of 394.6 $\mu\text{mol/g}$ is obtained with the P_4O_{10} weight percentage of 1.1 wt% under the illumination condition with IR only. The previous studies on using IR only for CO_2 reduction reported that the CO production rates ranged from 78 $\mu\text{mol/g}$ to 25 $\mu\text{mol/g}$.¹⁷⁻²¹ The CO production rate of 394.6 $\mu\text{mol/g}$ which achieved with P_4O_{10}/TiO_2 photocatalyst prepared by this study is 5 times as large as that in the previous studies. Therefore, it can be conducted that the P_4O_{10}/TiO_2 photocatalyst could significantly improve the CO production rate for CO_2 reduction with IR illumination only.

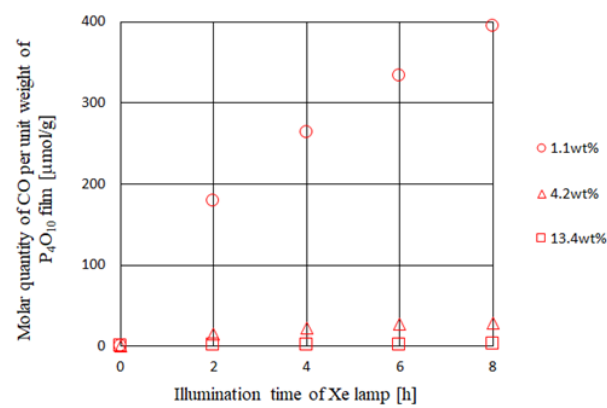


Figure 18 Comparison of molar quantity of CO per unit weight of P_4O_{10}/TiO_2 film among different weight percentages of P_4O_{10} within P_4O_{10}/TiO_2 film under the illumination condition with IR only.

However, the CO_2 reduction performance with P_4O_{10}/TiO_2 under the illumination condition with IR only is thought to be still low. To further improve the performance, other types of P for loading into TiO_2 , e.g., BP may be attempted. According to the previous report,²² the composite photocatalyst of BP and $g-C_3N_4$ has performed the H_2 production from H_2O under VIS and near IR illumination condition. P has a layer structure absorbing the light whose wavelength is ranged from UV to IR.

Conclusion

The impact of the amount of P_4O_{10} loaded on TiO_2 and the molar ratio of CO_2/H_2O on the CO_2 reduction performance under various illumination conditions have been studied in this paper. Based on the study, the following conclusions can be drawn:

- (1) The coated P_4O_{10}/TiO_2 film having teeth-like shape was formed on the netlike glass fiber irrespective of the weight percentage of P_4O_{10} within P_4O_{10}/TiO_2 film. The distribution of P_4O_{10} is more uniform under the small loading amount of P_4O_{10} .
- (2) This study revealed that the light absorption performance of TiO_2 film could be extended to VIS and IR wavelength by loading P_4O_{10} irrespective of the weight percentage of P_4O_{10} .
- (3) The CO_2 reduction performance for the CO_2/H_2O molar ratio of 1:1 was the highest among different molar ratios under the illumination condition with UV + VIS + IR, VIS + IR, and

IR only irrespective of the weight percentage of P_4O_{10} . This result matches with the theoretical molar ratio to produce CO according to the reaction scheme of CO_2/H_2O for TiO_2 .

- (4) The CO_2 reduction performance for the weight percentage of P_4O_{10} of 1.1 wt% was the highest among different weight percentages of P_4O_{10} under the illumination condition with UV + VIS + IR, VIS + IR, and IR only. The uniform distribution of P_4O_{10} can construct the fine network with TiO_2 .
- (5) Under the illumination condition with IR only, the molar quantity of CO per unit weight of P_4O_{10}/TiO_2 film of 394.6 $\mu\text{mol/g}$ was obtained, which is 5 times as large as that ever achieved before.

Funding details

JSPS KAKENHI.

Acknowledgements

The authors would like to gratefully thank from JSPS KAKENHI Grant Number JP21K04769 for the financial support of this work.

Conflicts of interests

The authors declare that there is no conflict of interest regarding the publication of this paper.

References

1. Global Monitoring Laboratory. 2022.
2. Jesic D, Jurkovic LD, Pohar A, et al. Engineering photocatalytic and photoelectrocatalytic CO_2 reduction reactions: mechanisms, intrinsic kinetics, mass transfer resistances, reactors and multi-scale modeling simulations. *Chemical Engineering Journal*. 2021;407.
3. Razzaq A, Ali S, Asif M, et al. Layered double hydroxide (LDH) based photocatalysts: an outstanding strategy for efficient photocatalytic CO_2 reduction. *Catalysts*. 2020;10.
4. Matavos-Aramyan S, Soukhakian S, Jazebizadeh MH, et al. On engineering strategies for photoselective CO_2 reduction – a through review. *Applied Materials Today*. 2020;18.
5. Abdullah H, Khan MMR, Ong HR, et al. Modified TiO_2 photocatalyst for CO_2 photocatalytic reduction: an overview. *Journal of CO_2 Utilization*. 2017;(22):15–32.
6. Remiro-Buenamanana S, Garcia H. Photoassisted CO_2 conversion into fuels. *Chem Cat Chem Minirev*. 2019;(11):342–356.
7. Zhu S, Chen X, Li Z, et al. Cooperation between inside and outside of TiO_2 : lattice Cu^+ accelerates carrier migration to the surface of metal copper for photocatalytic CO_2 Reduction. *Applied Catalysis B: Environmental*. 2020;264.
8. Jeong S, Kim GM, Kang GS, et al. Selectivity modulated by surface ligands on Cu_2O/TiO_2 catalysts for gas-phase photocatalytic reduction of carbon dioxide. *The Journal of Physical Chemistry C*. 2019;(123):29184–29191.
9. Jiang Z, Sun W, Miao W, et al. Living atomically dispersed Cu ultrathin TiO_2 nanosheet CO_2 reduction photocatalyst. *Advanced Sciences*. 2019;6.
10. Wang ZW, Shi YZ, Liu C, et al. Cu^+-Ti^{3+} Interface interaction mediated CO_2 coordination model for controlling the selectivity of photocatalytic reduction CO_2 . *Applied Catalysis B: Environmental*. 2022;301.
11. Su KY, Chen C Y, Wu R J. Preparation of Pd/TiO_2 nanowires for the photoreduction of CO_2 into renewable hydrocarbon fuels. *Journal of the Taiwan Institute of Chemical Engineers*. 2019;(96):409–418.
12. Camarillo R, Toston S, Martinez F, et al. Enhancing the photocatalytic reduction of CO_2 through engineering of catalysts with high pressure technology: Pd/TiO_2 photocatalysts. *The Journal of Supercritical Fluids*. 2017;(123):18–27.
13. Yu Y, Lan Z, Guo L, et al. Synergetic effects of Zn and Pd species in TiO_2 towards efficient photo-reduction of CO_2 into CH_4 . *New J Chem*. 2018;(42):483–488.
14. Zhao Y, Wei Y, Wu X, et al. Graphene-wrapped Pt/TiO_2 photocatalysts with enhanced photogenerated charges separation and reactant adsorption for high selective photoreduction of CO_2 to CH_4 . *Applied Catalysis B: Environmental*. 2018;(226):360–372.
15. Toston S, Camarillo R, Martinez F, et al. Supercritical synthesis of platinum-modified titanium dioxide for solar fuel production from carbon dioxide. *Chinese Journal of Catalysis*. 2017;(38):636–650.
16. Wei Y, Wu X, Zhao Y, et al. Efficient photocatalysts of TiO_2 nanocrystals-supported PtRu alloy nanoparticles for CO_2 reduction with H_2O : synergistic effect of Pt–Ru. *Applied Catalysis B: Environmental*. 2018;(236):445–457.
17. Hong LF, Guo R T, Yuan Y, et al. Urchinlike $W_{18}O_{49}/g-C_3N_4$ Z-scheme heterojunction for highly efficient photocatalytic reduction of CO_2 under full spectrum light. *Energy Fuels*. 2021;(35):11468–11478.
18. Dai W, Yu J, Luo S, et al. WS_2 quantum dots seeding in Bi_2S_3 nanotubes: a novel vis–NIR light sensitive photocatalyst with low–resistance junction interface for CO_2 reduction. *Chemical Engineering Journal*. 2020;389.
19. Gan J, Wang H, Hu H, et al. Efficient synthesis of tunable band-gap $CuInZnS$ decorated $g-C_3N_4$ hybrids for enhanced CO_2 photocatalytic reduction and near-infrared– triggered photodegradation performance. *Applied Surface Science*. 2021;564.
20. Yu M, Lv X, Idris AM, et al. Upconversion nanoparticles coupled with hierarchical $ZnIn_2S_4$ nanorods as a near-infrared responsive photocatalyst for photocatalytic CO_2 reduction. *Journal of Colloid and Interface Science*. 2022;(612):782–791.
21. Lu C, Li X, Li J, et al. Nonmetallic surface plasmon resonance coupling with pyroelectric effect for enhanced near-infrared-driven CO_2 reduction. *Chemical Engineering Journal*. 2022;445.
22. Zhu M, Kim S, Mao L, et al. Metal-free photocatalyst for H_2 evolution in visible to near-infrared region: black phosphorus/graphitic carbon nitride. *Journal of The American Chemical Society*. 2017;(139):13234–13242.
23. Kaushik R, Singh PK, Halder A. Modulation strategies in titania photocatalyst for energy recovery and environmental remediation. *Catalysis Today*. 2022;(384–386):45–69.
24. Nahar S, Zain MFM, Kadhum AAH, et al. Advances in photocatalytic CO_2 reduction with water: A Review. *Materials*. 2017;(10):629.
25. Tahir M, Amin NS. Advances in visible light responsive titanium oxide based photocatalysts for CO_2 conversion to hydrocarbon fuels. *Energy Convers Manag*. 2013;(76):194–214.
26. Goren Z, Willner I, Nelson AJ. Selective photoreduction of CO_2/HCO_3^- to formate by aqueous suspensions and colloids of Pd/TiO_2 . *J Physic Chem*. 1990;(94):3784–3790.
27. Tseng IH, Chang W C, Wu J CS. Photoreduction of CO_2 using sol–gel derived titania and titania-supported copper catalysts. *Appl Catal B*. 2002;(37):37–38.
28. Izumi Y. Recent Advances in the photocatalytic conversion of carbon dioxide to fuels with water and/or hydrogen using solar energy and beyond. *Coord Chem Rev*. 2013;(257):171–186.
29. Nishimura A, Ishida N, Tatematsu D, et al. Effect of Fe loading condition and reductants on CO_2 reduction performance with Fe/TiO_2 Photocatalyst. *Int J Photoenergy*. 2017;2017.

30. Nishimura A, Sakakibara Y, Inoue T, et al. Impact of molar ratio of NH_3 and H_2O on CO_2 reduction performance over Cu/TiO_2 photocatalyst. *Phys Astron Int J*. 2019;(3):176–182.
31. Nishimura A, Sakakibara Y, Koshio A, et al. The impact of amount of Cu on CO_2 reduction performance of Cu/TiO_2 with NH_3 and H_2O . *Catalysts*. 2021:11.
32. Nishimura A, Shimada R, Sakakibara Y, et al. Comparison of CO_2 reduction performance with NH_3 and H_2O between Cu/TiO_2 and Pd/TiO_2 . *Molecules*. 2021:26.
33. Japan Science and Technology Agency, J-STORE. P2009–184861A. 2022.
34. Nishimura A, Mitsui G, Nakamura K, et al. CO_2 reforming characteristics under visible light response of Cr- or Ag-doped TiO_2 prepared by sol-gel and dip-coating process. *International Journal of Photoenergy*. 2012.
35. Japan Society of Mechanical Engineering. Heat Transfer Hand Book, 1st ed.; Maruzen: Tokyo, Japan. 1993:367–369.
36. Jiang L, Yang J, Zhou S, et al. Strategies to extend near-infrared light harvest to polymer carbon nitride photocatalysts. *Coordination Chemistry Reviews*. 2021:439.